Supporting Information

Revealing Charge Transport Mechanisms in Li_2S_2 for Li-Sulfur Batteries

Zhixiao Liu,[1] Perla B. Balbuena,[2,*] Partha P. Mukherjee[1,*]

[1]Department of Mechanical Engineering, Texas A&M University, College Station, Texas 77843, USA

[2]Department of Chemical Engineering, Texas A&M University, College Station, Texas 77843, USA

[*]*Correspondence*: pmukherjee@tamu.edu (P. P. Mukherjee); balbuena@tamu.edu (P. B. Balbuena)

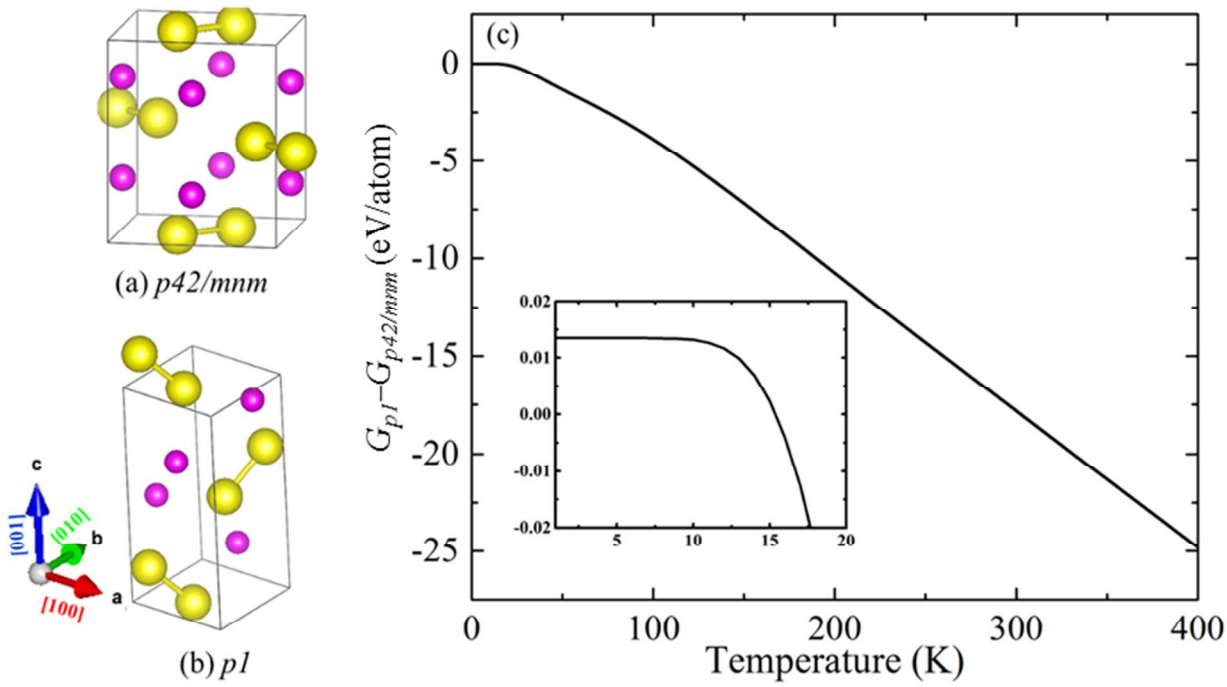

Figure S1. Crystal structures of Li_2S_2 with (a) *p42/mnm* space group and (b) *p1* space group. The *p42/mnm* structure was predicted by Yang *et al.*, and the *p1* structure was predicted by Feng *et al.*. (c) The Gibbs energy difference of *p1* Li_2S_2 and *p42/mnm* Li_2S_2 as a function of temperature. The structure with *p1* space group is more stable at room temperature.

The method reported by Siegel and collaborators is employed to calculate the Gibbs free energy.[1] The Gibbs free energy and enthalpy are calculated by

$$G(T) = H(T) - TS_{vib}(T), \tag{S1}$$

$$H(T) = E + H_{vib}(T). \tag{S2}$$

Here E is the energy of the system at the first-principles condition (0 K). Vibrational contributions to the entropy and enthalpy are expressed as

$$S_{vib}(T) = \sum \frac{\frac{\hbar\omega_i}{\kappa T}}{\exp\left(\frac{\hbar\omega_i}{\kappa T}\right)} - \ln\left[1 - \exp\left(-\frac{\hbar\omega_i}{\kappa T}\right)\right], \tag{S3}$$

$$H_{vib}(T) = \sum \frac{1}{2}\hbar\omega_i + \hbar\omega_i\left[\exp\left(\frac{\hbar\omega_i}{\kappa T}\right) - 1\right]^{-1}. \tag{S4}$$

In Eqns. S3 and S4, $\hbar$ is Planck constant divided by 2π, and κ is the Boltzmann constant.

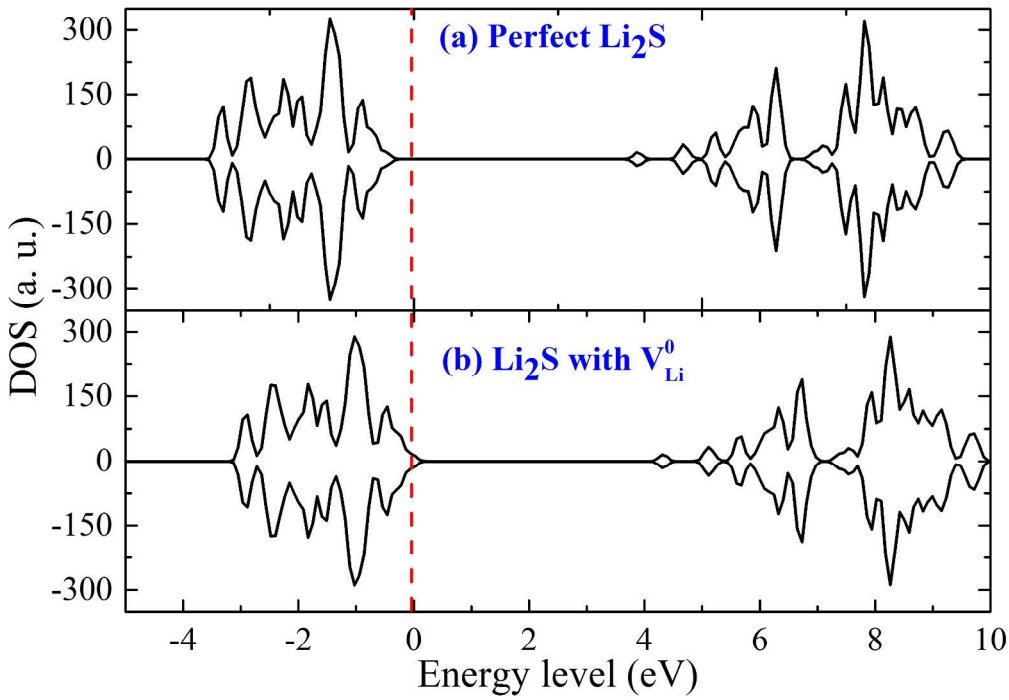

Figure S2. Total density of states (TDOS) of (a) perfect Li_2S crystal and (b) Li_2S with a neutral Li vacancy. The neutral Li vacancy is generated by removing a Li atom from a (3×3×3) supercell

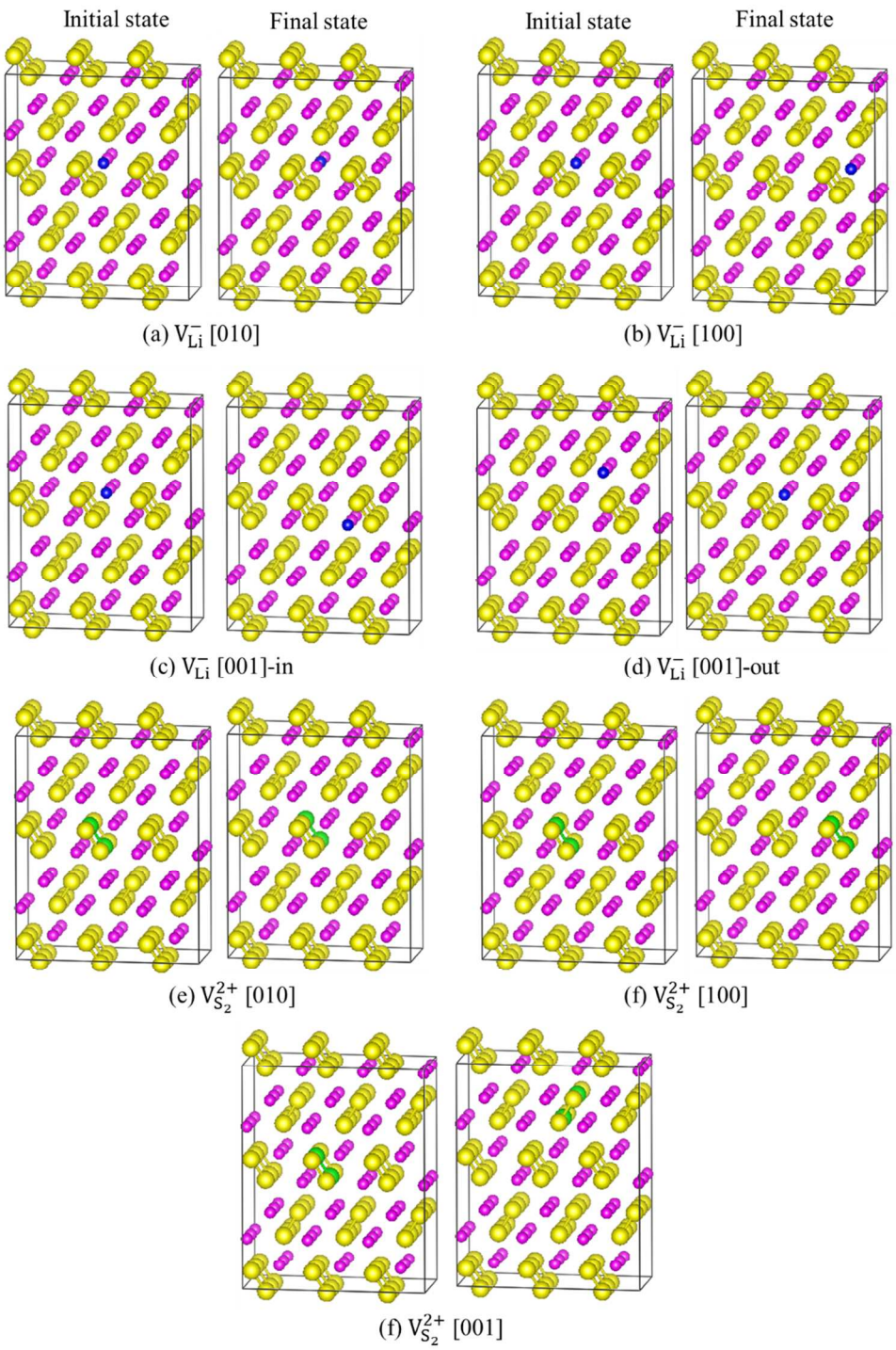

Figure S3. Schematic illustration of initial and final states of the proposed diffusion paths. Violet spheres represent Li atoms, and yellow spheres represent sulfur atoms, respectively. Blue spheres represent Li vacancies, and green spheres represent S_2 vacancies, respectively. For both Li vacancy and S_2 vacancy diffusion, [001] diffusion paths are not exactly parallel to the [001] axis. Proposed polaron diffusion paths are the same as S_2 vacancy diffusion paths

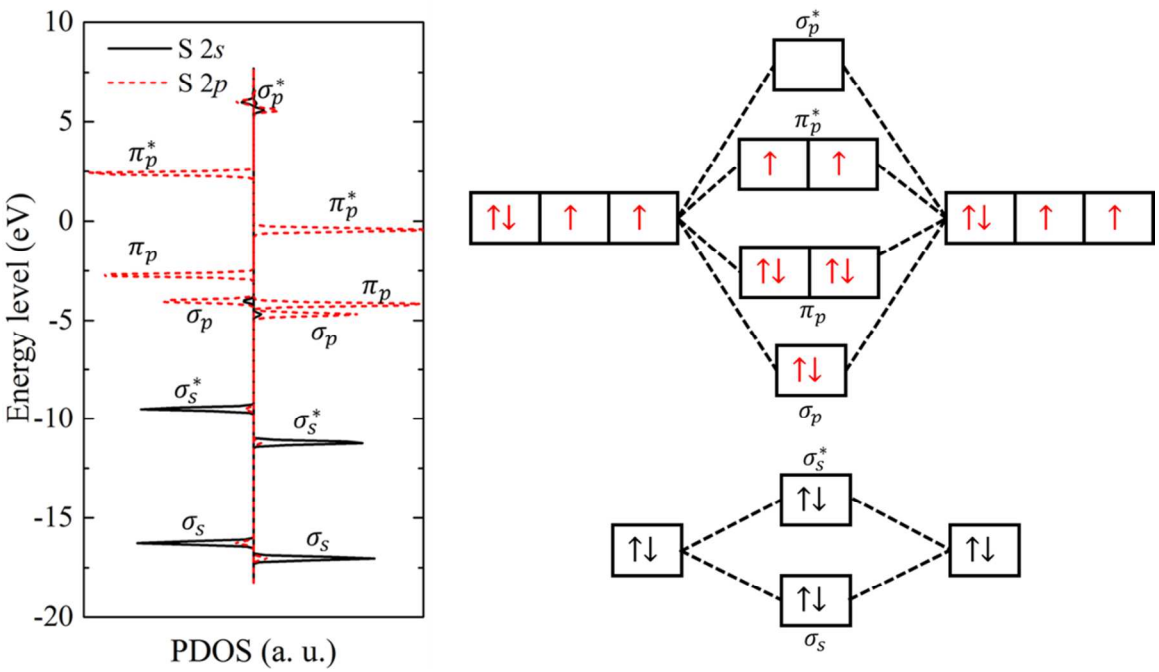

Figure S4. Projected density of states (PDOS) of an isolated S_2 molecule and the schematic illustration of the S_2 molecular orbitals.

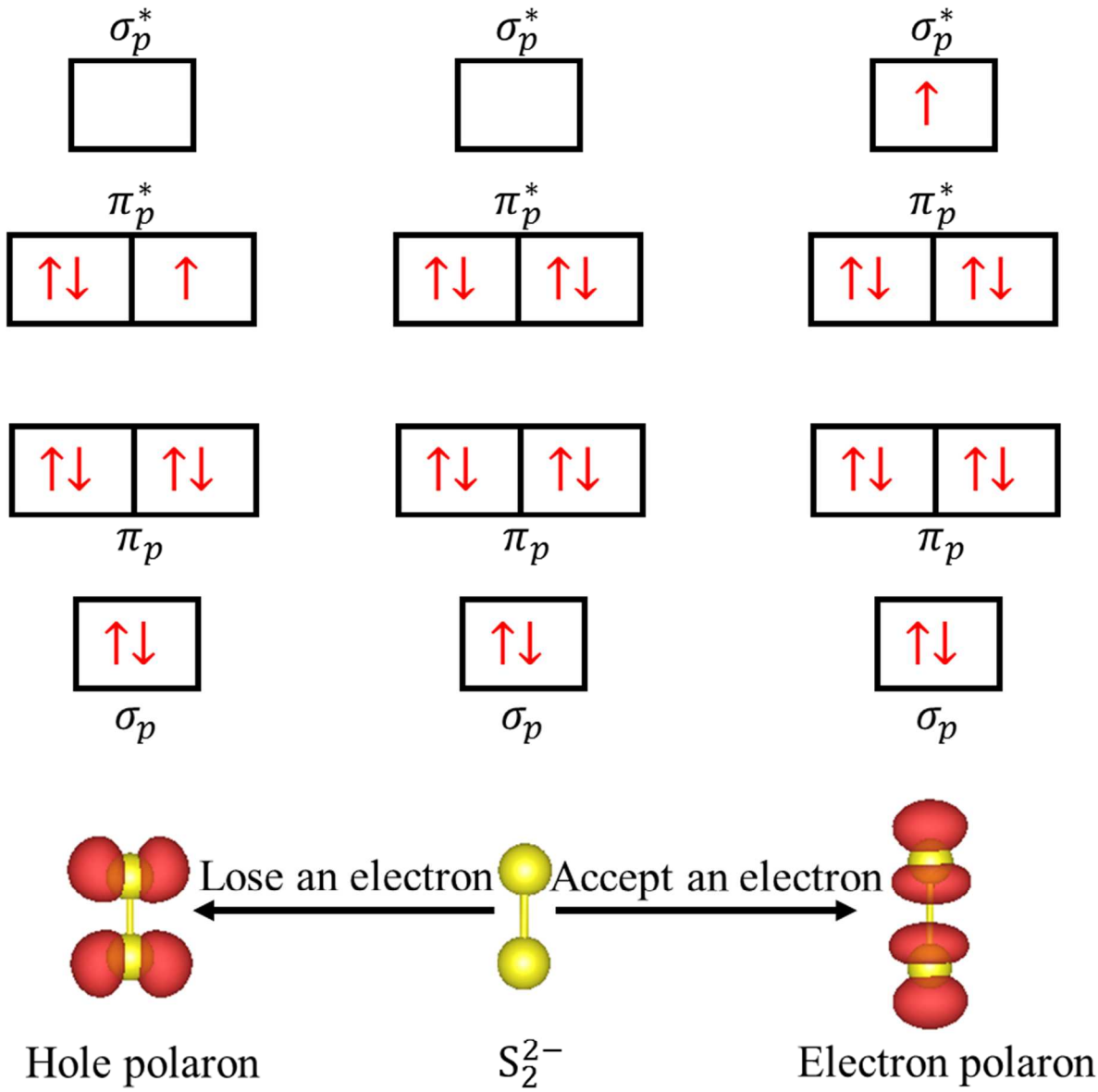

Figure S5. Schematic illustration of the mechanism of forming a hole polaron and an electron polaron.

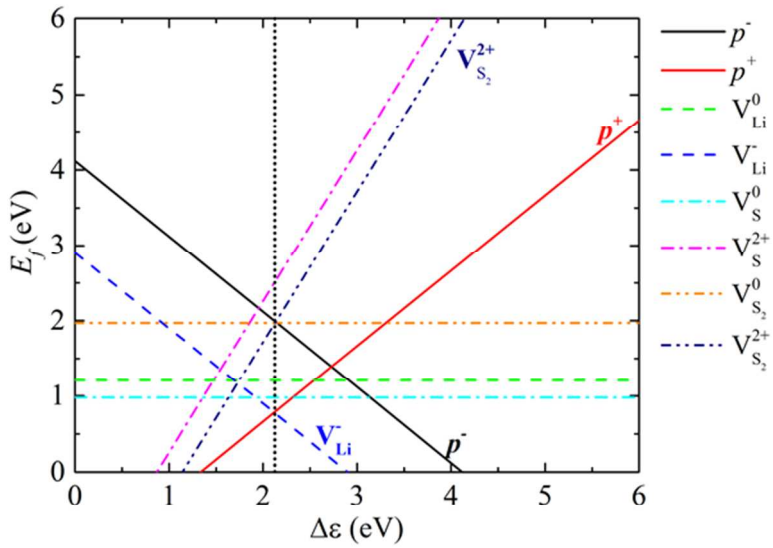

(a) With Makov-Payne correction

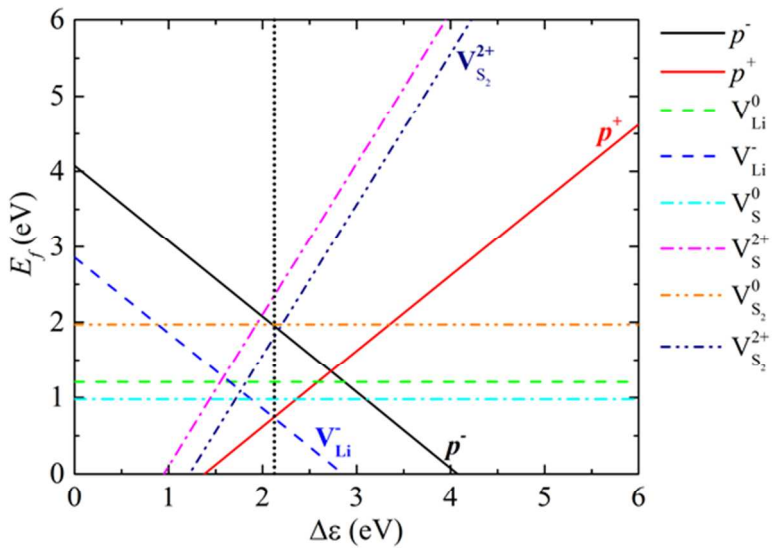

(b) Without Makov-Payne correction

Figure S6. Formation energies of native defects in Li_2S_2 calculated (a) with considering Makov-Payne correction and (b) without considering Makov-Payne correction.

The formation energy was calculated by

$$E_f(X^q) = E(X^q) - E^0 - \sum_i n_i g_i + q_i \Delta\epsilon + E_{MP}. \quad \text{(S5)}$$

Here $E(X^q)$ was the total energy of the system with a charged defect, E^0 was the total energy of perfect Li_2S_2, g was the chemical potential of species i. In Eqn. S5, i denote Li^+ cation or S_2^{2-} anion. The symbol $\Delta\epsilon$ represented Fermi level referencing to VBM as $\Delta\epsilon = \epsilon_F - \epsilon_{VBM}$, and q

was the charge number of the defect. To avoid interaction energy of defects between two consecutive images, the total energy of the system was calculated based on a (3×3×2) supercell with Γ-only k-point. The criteria for structure relaxing is set -0.02 eV Å^{-1}. The Makov-Payne correction (E_{MP} term in Eqn. S5) was also considered to estimate the interaction between charge images.[2-3] According to the present DFT simulation, the components of the dielectric tensor along a, b and c directions are $\epsilon_{aa} = 4.28$, $\epsilon_{bb} = 5.44$ and $\epsilon_{cc} = 5.37$. The MP correction for Li_2S_2 is 0.02 eV for (3×3×2) supercell with $q = \pm 1$. The chemical potential of Li is calculated from the equilibrium potential for forming Li_2S_2 ($\phi_0 = 2.2$ V):

$$g_{Li} = E_{Li}^{bcc} - e\phi, \tag{S6}$$

and the chemical potential of S_2 is calculated by

$$g_{S_2} = E_{Li_2S_2} - g_{Li}. \tag{S7}$$

E_{Li}^{bcc} is the energy of a Li atom in the *bcc* structure, and $E_{Li_2S_2}$ is the energy of Li_2S_2 per unit.

In the present study, the Fermi level for the formation energy calculation (Eqn. S5) is a hypothetical Fermi level, which is the energy level that makes the system satisfy charge neutrality. This approach was employed by Siegel and collaborators to investigate charge carrier concentration in crystalline Li_2O_2.[4-5] It is worth noticing that the relative position of the VBM to the Fermi level ($\Delta\epsilon$) is dependent on the applied potential Φ as reported by Luntz and collaborators.[6-8] The applied potential-dependent Fermi level can be aligned by either metal-insulator-metal (MIM) modeling[7-8] or using experimental values.[6] Using this alignment approach, Luntz *et al*. found that the Fermi level in Li_2O_2 is ~0.35 eV above the VBM at the equilibrium potential ($\Delta\epsilon(\Phi_0) = 0.35$ eV). The Fermi level reported by Luntz *et al.* is closer to the VBM than the value ($\approx$ 2 eV) reported by Siegel *et al.*[4] According to Eqn. S5, a lower Fermi level can reduce the formation energy of a positively charged hole polaron, and increase the formation energy of a negatively charged Li vacancy. It can be inferred that the current study about Li_2S_2 may underestimate the electronic conductivity and overestimate the ionic conductivity.

The applied potential ϕ between the Li_2S_2 product and the Li anode is considered in the present study as shown in Eqn. S6. In this study, the equilibrium potential $\phi_0 = 2.2$ eV is used to estimate the formation energies of charged defects. At the equilibrium potential Φ_0 of $\mathrm{Li + S \leftrightarrow Li_2S_2}$ electrochemical system, the Fermi level is common throughout all species in the battery as $\epsilon_F(\Phi_0) = g_{Li}(\Phi_0)$. Therefore, $\Phi_0 = 2.2$ V is the most appropriate potential for describing the chemistry of charged defects.[8]

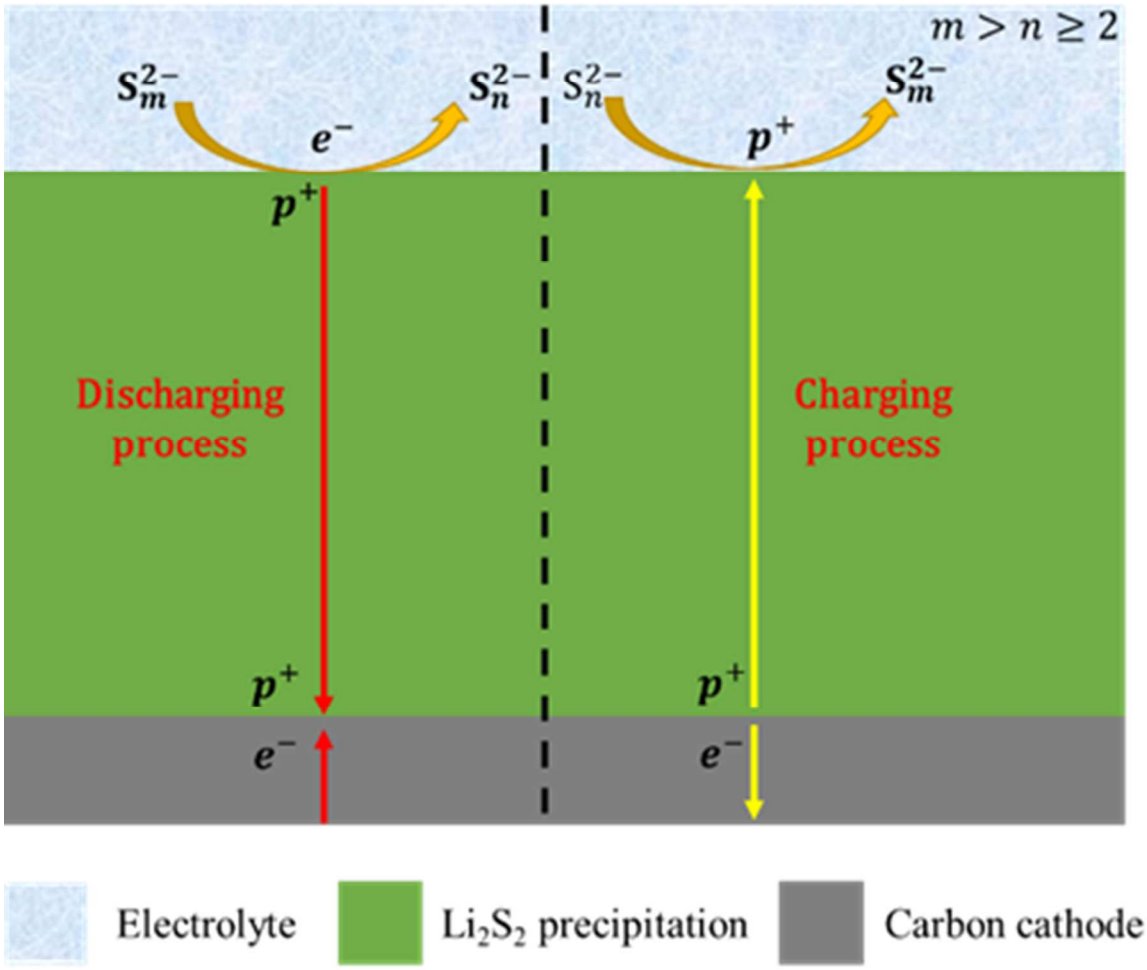

Figure S7. Schematic illustration of hole polaron transport during charging/discharging processes.

References

(1) Park, H.; Koh, H. S.; Siegel, D. J. First-Principles Study of Redox End Members in Lithium–Sulfur Batteries. *J. Phys. Chem. C* **2015,** *119*, 4675-4683.

(2) Makov, G.; Payne, M. Periodic Boundary Conditions in Ab Initio Calculations. *Phys. Rev. B* **1995,** *51*, 4014.

(3) Komsa, H.-P.; Rantala, T. T.; Pasquarello, A. Finite-Size Supercell Correction Schemes for Charged Defect Calculations. *Phys. Rev. B* **2012,** *86*, 045112.

(4) Radin, M. D.; Siegel, D. J. Charge Transport in Lithium Peroxide: Relevance for Rechargeable Metal–Air Batteries. *Energy Environ. Sci.* **2013,** *6*, 2370-2379.

(5) Radin, M. D.; Monroe, C. W.; Siegel, D. J. How Dopants Can Enhance Charge Transport in Li_2O_2. *Chem. Mater.* **2015,** *27*, 839-847.

(6) Luntz, A. C.; Viswanathan, V.; Voss, J.; Varley, J. B.; Nørskov, J. K.; Scheffler, R.; Speidel, A. Tunneling and Polaron Charge Transport through Li_2O_2 in Li–O_2 Batteries. *J. Phys. Chem. Lett.* **2013,** *4*, 3494-3499.

(7) Viswanathan, V.; Thygesen, K. S.; Hummelshøj, J.; Nørskov, J. K.; Girishkumar, G.; McCloskey, B.; Luntz, A. Electrical Conductivity in Li_2O_2 and Its Role in Determining Capacity Limitations in Non-Aqueous Li-O_2 Batteries. *J. Chem. Phys.* **2011,** *135*, 214704.
(8) Varley, J.; Viswanathan, V.; Nørskov, J.; Luntz, A. Lithium and Oxygen Vacancies and Their Role in Li_2O_2 Charge Transport in Li–O_2 Batteries. *Energy Environ. Sci.* **2014,** *7*, 720-727.